EXPERIMENTAL VERIFICATION OF THE INSIDE INTEGRATION METHOD (IIM) FOR THE SIMULATION OF SHALLOW WATER FLOW RUNNING ONTO A SLOPING GROUND

Md. Abdul Aziz [(1)], Md Sohail Us Samad [(2)], Upal Mahamud [(3)], Md Nurul Huda [(4)]

Military Institute of Science and Technology [(1,2,4)]
Institute of Water Modeling [(3)]

This study shows the validation of a new numerical scheme with hydraulic experiment. The proposed scheme is a new computational scheme to solve shallow-water equations for surface waves shoaling on a slope. Experiment was carried out in a wave tank set on an oscillating bed, which can be moved, uniformly equal in both directions. Used flume had a flat bed of 50.5 cm and having a constant slope of 11.3^0 in one end whereas the other end is fixed with a vertical wall. As initial condition, water depth was 2cm, wave period was 3.5 s and the movement of the oscillating bed was 6 cm. From the comparisons of the time variation of the moving boundary and the water level along the tank, numerical computation was found to provide good agreement with laboratory experiments.

Keywords: Moving boundary, Numerical Computation, Wave Shoaling, Hydraulic experiment

1. INTRODUCTION

The behavior of long-wave shoaling on sloping beaches has received intensive study by many scientists and engineers. Primary impacts of the behavior of wave shoaling with a moving boundary are inundation in the form of tsunamis and storm surge, causing exacerbation of flooding and beach erosion. These impacts, in turn, cause higher ordered impacts in a wide range of coastal system. Since there exist highly productive ecosystems, large portion of the world population, and intensive socioeconomic activities in the coastal zone, it is crucial to predict the degree and range of the possible impacts of wave shoaling in a wide coastal area.

Several studies had been carried out to solve shallow-water equations to waves shoaling on a slope. Carrier and Greenspan (1958) derived a nonlinear transformation from Stoker non-linear theorem to reduce the two equations to a single linear equation and solved several initial value problems. But the analytical solution is obtained under some simplifications, like a uniform slope. The approach can solve some initial value problems, which is not conclusive for all the cases of wave shoaling.

Eulerian scheme is used in the time varying fluid domain in the past. The common practice was either use wet-dry interface or a coordinate transformation technique. Gopalakrishnan and Tung (1983) developed a finite element model for one horizontal dimension, whish used a fixed grid, except at the coastline where an element was allowed to deform to follow the shoreline and to split into two elements if it became too stretched. Some other implementation of fixed grid method can be found in Liu et al. (1995) and Balzano (1998). These methods determine the position of the shoreline as one of the fixed grid points, which means shoreline is moved one or more Δx at a time. This makes the wet-dry methods more prone to instabilities.

Most of the models used Lagrangian frame of scheme use fixed computational grid exclusively since the independent variables are the initial coordinates of the fluid particles, the computational grid does not distort, even as the shoreline moves that is the motivation for performing the computation in this frame of reference. Zelt and Raichlen (1989) describe a finite element technique to study the propagation of long waves in two dimensions in regions of arbitrary shape with vertical or shopping boundaries.

DeSilva et al. (1996) include effect of surface tension, in his model. R.S.Prasad, I.A. Svendsen (2003) used two different ways to solve in two steps, the first is to establish an equation that determines the motion of the shoreline based on the local momentum balance then to develop and implement into a shoreline model the capability of accommodating a changing computational domain.

Ishikawa et al. and Nakayama et al. proposed a new computational algorithm where hydraulic boundary conditions are taken as constraint conditions at the moving shoreline at fixed regular grid and partially integrating the weighted residual equations to deduce its weak form in which the constraint conditions are embodied. Detail of the model is given in the succeeding chapter.

2. MODEL DESCRIPTION

2.1 Governing equations

Assuming the uniformity of horizontal velocity (in a water column) and the hydrostatic pressure, we obtain shallow-water Equations (1) and (2), in which Equation (1) is the equation of continuity and Equation (2) is the momentum equation.

$$\frac{\partial h}{\partial t}+\frac{\partial (uh)}{\partial x}=0 \quad (1)$$

$$\frac{\partial u}{\partial t}+u\frac{\partial u}{\partial x}+g\frac{\partial (h+z)}{\partial x}=0 \quad (2)$$

Where t is time, x is the distance toward the shore, h is the water depth, z is the bed elevation and u is the water velocity in x direction.

2.2. Time splitting

In a numerical simulation of wave shoaling, accurate estimation of the shoreline motion, which coincides with the water particle, is important essentially. Accordingly, Lagrangean tracing of the shoreline motion will be implemented more easily by introducing the "time splitting" of the governing equations because the procedure of tracing can be included in the advection phase calculation of flow field.

Non-advection phase

$$\frac{\tilde{h}-h^n}{\Delta t}+h\frac{\partial u}{\partial x}=0 \quad (3)$$

$$\frac{\tilde{u}-u^n}{\Delta t}+g\frac{\partial (h+z)}{\partial x}=0 \quad (4)$$

Advection phase

$$\frac{h^{n+1}-\tilde{h}}{\Delta t}+\tilde{u}\frac{\partial \tilde{h}}{\partial x}=0 \quad (5)$$

$$\frac{u^{n+1}-\tilde{u}}{\Delta t}+\tilde{u}\frac{\partial \tilde{u}}{\partial x}=0 \quad (6)$$

2.3 Calculation of non-advection phase

2.3.1 Shape and weight functions

To satisfy the boundary condition on a moving boundary, the finite-element method is applied to solve advection phase. For an element with a moving boundary, linear or higher order functions have to be used as shape and weight functions to include the condition on a moving boundary. In this paper, we decided to apply linear function as shape and weight functions.

[Shape Function]

$$\psi_l(\xi)=(1-\xi)=\tilde{\phi}_1(\xi),\psi_r(\xi)=\xi=\tilde{\phi}_2(\xi) \quad (7)$$

Where ξ is a local coordinate in an element $\xi=(x-x_i)/\Delta x$, $\Delta x=x_{i+1}-x_i$ is the length of element and x_i and x_{i+1} is the locations of the left and right ends of the element, respectively.

[Weight Function]

For an element with a moving boundary, we decided to use linear function as weight function. In contrast to an element with a moving boundary, it is not needed for an element filled with water to be solved with linear function as weight function because there are no moving boundaries and using simpler weight function enables computation time to be shortened. Delta function is, thus, applied to an element filled with water.

For element filled with water

$$w_l(\xi)=\delta(\xi)=\bar{\phi}_1(\xi),w_r(\xi)=\delta(1-\xi)=\bar{\phi}_2(\xi) \quad (8)$$

For elements on the moving boundary

$$w_l(\xi)=w_l(\xi)=(1-\xi)=\tilde{\phi}_1(\xi),w_r(\xi)=\xi=\tilde{\phi}_2(\xi),(1-\xi)=\bar{\phi}_2(\xi) \quad (9)$$

Elementary matrix for inside water elements

Substitution of Equations (7) to (9) into Equations (3) yields

$$\sum_{j=1}^{2}\Delta\tilde{H}_j\int_0^1\tilde{\phi}_j\bar{\phi}_i d\xi\approx-\frac{\Delta t}{\Delta x}\sum_{j=1}^{2}\sum_{k=1}^{2}\tilde{H}_j{}^n\tilde{U}_k{}^n \quad (10)$$
$$\int_0^1\tilde{\phi}_j\frac{\partial\bar{\phi}_k}{\partial\xi}\bar{\phi}_i d\xi$$

Where

$$h=\sum_{j=1}^{2}\tilde{H}_j{}^n\tilde{\phi}_j(\xi) \quad (11)$$

$$u=\sum_{j=1}^{2}\tilde{U}_j{}^n\tilde{\phi}_j(\xi) \quad (12)$$

$$z=\sum_{j=1}^{2}\tilde{Z}_j{}^n\tilde{\phi}_j(\xi) \quad (13)$$

and $\tilde{H}_1 = h_i, \tilde{H}_2 = h_{i+1}, \tilde{U}_1 = u_i, \tilde{U}_2 = u_{i+1},$
$\tilde{Z}_1 = z_i, \tilde{Z}_2 = z_{i+1}.$

Equations (10) can be modified for an element filled with water as

$$\begin{vmatrix} 1/2 & 0 \\ 0 & 1/2 \end{vmatrix} \begin{bmatrix} \Delta\tilde{H}_1 \\ \Delta\tilde{H}_2 \end{bmatrix} = \frac{\Delta t}{2\Delta x} \begin{bmatrix} \tilde{H}_1^{\,n}(\tilde{U}_1^{\,n} - \tilde{U}_2^{\,n}) \\ \tilde{H}_2^{\,n}(\tilde{U}_1^{\,n} - \tilde{U}_2^{\,n}) \end{bmatrix} \quad (14)$$

In the same way for the momentum equation we can obtain the elementary equations.

$$\sum_{j=1}^{2} \Delta\tilde{U}_j \int_0^1 \tilde{\phi}_j \bar{\phi}_i d\xi = -g \frac{\Delta t}{\Delta x} \sum_{j=1}^{2} (\tilde{H}_j^{\,n} + \tilde{Z}_j) \int_0^1 \frac{\partial \bar{\phi}_j}{\partial \xi} \bar{\phi}_i d\xi \quad (15)$$

The matrix of the elementary Equations (15)

$$\begin{vmatrix} 1/2 & 0 \\ 0 & 1/2 \end{vmatrix} - \begin{bmatrix} \Delta\tilde{U}_1 \\ \Delta\tilde{U}_2 \end{bmatrix} = - \frac{\Delta t}{2\Delta x} g \begin{bmatrix} -(\tilde{H}_1^{\,n} + \tilde{Z}_1) + (\tilde{H}_2^{\,n} + \tilde{Z}_2) \\ -(\tilde{H}_1^{\,n} + \tilde{Z}_1) + (\tilde{H}_2^{\,n} + \tilde{Z}_2) \end{bmatrix} \quad (16)$$

Runge-kutta gill method was used for time integration.

2.3.2 For an element with a moving boundary

We used linear functions as shape and weight functions. Here we defined x_s to as the location of a moving boundary and integration is done in the area filled with water, $x_i \le x \le x_s$. (Figure 1)

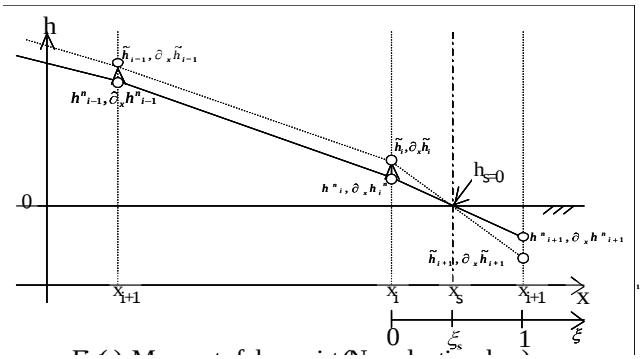

Figure 1. Movement of shoreline non-advection phase

The boundary condition at the moving boundary ($x=x_s$) is h=0. Equation (3) becomes

$$\sum_{j=1}^{2} \Delta\tilde{H}_j \int_0^{\xi_s} \tilde{\phi}_j \tilde{\phi}_i d\xi = -\frac{\Delta t}{\Delta x} \sum_{j=1}^{2} \sum_{k=1}^{2} \tilde{H}_j^{\,n} \tilde{U}_k^{\,n} \int_0^{\xi_s} \tilde{\phi}_j \frac{\partial \tilde{\phi}_k}{\partial \xi} \tilde{\phi}_i d\xi \quad (17)$$

Where ξ_s is the position of the shore point on the local coordinate ($= x_s / \Delta x$)

By taking a partial integral of the term of the right hand side, substituting the first boundary condition at $\xi = \xi_s$, and taking the return process, we get the weak form of weighted residual equation.

$$\sum_{j=1}^{2} \Delta\tilde{H}_j \int_0^1 \tilde{\phi}_j \tilde{\phi}_i d\xi = -\frac{\Delta t}{\Delta x} \sum_{j=1}^{2} \sum_{k=1}^{2} \tilde{H}_j^{\,n} \tilde{U}_k^{\,n} \int_0^1 \tilde{\phi}_j \frac{\partial \tilde{\phi}_k}{\partial \xi} \bar{\phi}_i d\xi + \frac{\Delta t}{\Delta x} [hu\tilde{\phi}_i]_{\xi=\xi_s} \quad (18)$$

Where, $\xi_s = (x_s - x_i)/\Delta x$

The above equation can be written in a matrix form

$$\begin{vmatrix} B_{11} & B_{12} \\ B_{21} & B_{22} \end{vmatrix} \begin{bmatrix} \Delta\tilde{H}_1 \\ \Delta\tilde{H}_2 \end{bmatrix} = \frac{\Delta t}{\Delta x} \begin{bmatrix} B_{13} \\ B_{23} \end{bmatrix} \quad (19)$$

Where the matrix elements are as follows

$$B_{11} = \xi_s - \xi_s^{\,2} + \frac{\xi_s^{\,3}}{3} \quad (20)$$

$$B_{12} = \frac{\xi_s^{\,2}}{2} - \frac{\xi_s^{\,3}}{3} \quad (21)$$

$$B_{21} = \frac{\xi_s^{\,2}}{2} - \frac{\xi_s^{\,3}}{3} \quad (22)$$

$$B_{22} = \frac{\xi_s^{\,3}}{3} \quad (23)$$

$$B_{13} = (1 - 2\xi_s + 2\xi_s^{\,2} - \frac{2\xi_s^{\,3}}{3})\tilde{U}_1^{\,n}\tilde{H}_1^{\,n} + (\xi_s - \frac{3\xi_s^{\,2}}{2} + \frac{2\xi_s^{\,3}}{3})\tilde{U}_1^{\,n}\tilde{H}_2^{\,n} + (-\xi_s^{\,2} + \frac{2\xi_s^{\,3}}{3})\tilde{U}_2^{\,n}\tilde{H}_1^{\,n} + (\frac{\xi_s^{\,2}}{2} - \frac{2\xi_s^{\,3}}{3})\tilde{U}_2^{\,n}\tilde{H}_2^{\,n} \quad (24)$$

$$B_{23} = (\xi_s - \frac{3\xi_s^{\,2}}{2} + \frac{2\xi_s^{\,3}}{3})\tilde{U}_1^{\,n}\tilde{H}_1^{\,n} + (\xi_s - \frac{2\xi_s^{\,3}}{3})\tilde{U}_1^{\,n}\tilde{H}_2^{\,n} + (\frac{\xi_s^{\,2}}{2} - \frac{2\xi_s^{\,3}}{3})\tilde{U}_2^{\,n}\tilde{H}_1^{\,n} + \frac{2\xi_s^{\,3}}{3}\tilde{U}_2^{\,n}\tilde{H}_2^{\,n} \quad (25)$$

In case of momentum Equation (4) from $x=x_i$ to $x=x_s$ gives

$$\sum_{j=1}^{2} \Delta\tilde{U}_j \int_0^{\xi_s} \tilde{\phi}_j \tilde{\phi}_i d\xi = -g \frac{\Delta t}{\Delta x} \sum_{j=1}^{2} (\tilde{H}_j^{\,n} + \tilde{Z}_j) \int_0^{\xi_s} \frac{\partial \tilde{\phi}_j}{\partial \xi} \tilde{\phi}_i d\xi \quad (26)$$

The matrix form of the equation (25)

$$\begin{vmatrix} A_{11} & A_{12} \\ A_{21} & A_{22} \end{vmatrix} \begin{bmatrix} \Delta\tilde{U}_1 \\ \Delta\tilde{U}_2 \end{bmatrix} = g \frac{\Delta t}{\Delta x} \begin{bmatrix} A_{13} \\ A_{23} \end{bmatrix} \quad (27)$$

Where, $B_{11}=A_{11}$, $B_{12}=A_{12}$, $B_{21}=A_{21}$, $B_{22}=A_{22}$ and

$$B_{13} = (-\xi_s + \frac{\xi_s^{\,2}}{2})(\tilde{H}_1^{\,n} + \tilde{Z}_1) + (\xi_s - \frac{\xi_s^{\,2}}{2})(\tilde{H}_2^{\,n} + \tilde{Z}_2) \quad (28)$$

$$B_{23} = -\frac{\xi_s^{\,2}}{2}(\tilde{H}_1^{\,n} + \tilde{Z}_1) + \frac{\xi_s^{\,2}}{2}(\tilde{H}_2^{\,n} + \tilde{Z}_2) \quad (29)$$

Construction of the set of overall equations

Total matrix is constructed from Equation 19 and Equation 27 the total matrix become as below

$$\begin{vmatrix} 1/2 & 0 & & & & \\ 0 & 1 & & & & \\ & \cdot & & & & \\ & & \cdot & & & \\ & & & 1 & & \\ & & & \cdot & 5/6 & 1/6 \\ & & & & 1/6 & 1/3 \end{vmatrix} \begin{vmatrix} \dot{U}_1 \\ U_2 \\ \cdot \\ \dot{U}_i \\ \cdot \\ U_{N-1} \\ U_N \end{vmatrix} = \begin{vmatrix} 1/2\{(H_1+F_1)-(H_2+F_2)\} \\ 1/2\{(H_1+F_1)-(H_3+F_3)\} \\ \cdot \\ 1/2\{(H_{i-1}+F_{i-1})-(H_{i+1}+F_{i+1})\} \\ \cdot \\ 1/2\{(H_{N-2}+F_{N-2})-(H_N+F_N)\} \\ 1/2\{(H_{N-1}+F_{N-1})-(H_N+F_N)\} \end{vmatrix} \quad (30)$$

2.3.3 Calculation for advection phase

In the advection calculation, the water surface elevation is changed through the process of conventional CIP at each grid point in the water (x_i). Simultaneously, the moving boundary (x_s) moves. Water depth at the outside grid point (x_{i+1}) is extrapolated from the values at x_i and x_s. Velocity field is also shift in the same way. Velocity interpolated from the values at x_i and x_{i+1}.

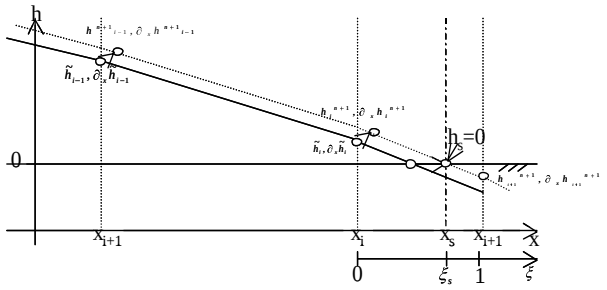

Figure 2.Movement of shore line advection phase.

Modeling of wave breaking to shallow-water equations

Because wave nonlinearity is not large in this study, linear mild-slope assumptions by Watanabe and Dibajnia (1988) may be applied to this problem. The simplified damping term due to wave breaking in shallow-water equations is given as

$$\frac{\partial u}{\partial t} + u\frac{\partial u}{\partial x} = -g\frac{\partial h}{\partial x} - \frac{M_D}{h} \quad (31)$$

$$M_D = \alpha_D s\sqrt{\frac{g}{h}uh} \quad (32)$$

Where M_D is the damping term α_D (damping co-efficient) is 2.5 and s is the gradient of slope. Using bottom friction enables the second term in the right hand side of Equation (32) to define as

$$\frac{M_D}{h} = f_{bottom}\frac{u^2}{h} \quad (33)$$

From Eq. (31) and (32)

$$\alpha_D s\sqrt{\frac{g}{h}}u = f_{bottom}\frac{u^2}{h} \quad (34)$$

$$\alpha_D s\frac{\sqrt{gh}}{u} = f_{bottom} \quad (35$$

Wave breaking is considered to occur when the horizontal velocity is larger than wave speed, which corresponds to that the Froude number is more than 1. Because wave breaking disables shallow-water assumption to be satisfied, the Froude number may be
assumed to be 1 in a wave-breaking zone to apply shallow water equations to this problem.

$$f_{bottom} = \alpha_D s \quad (36)$$

In numerical computations, we define the wave-breaking zone as the area from the wave-breaking point toward inshore and use Equation (35) to model wave breaking in a wave-breaking zone. Experimental works in this study are followed from the succeeding section.

3. EXPERIMENTAL WORKS

3.1. Experimental set up

Extensive experiments had been carried out for checking the position of moving boundary and the flow profile at the time of run up and run down flow on a sloping beach. Figure 3 shows the dimensional sketch of the experiment set up.

The wave tank is 2 meter long, 0.7m high and 0.3 m wide, which is equipped with a motor that is controlled by a computer. The bottom bed of the wave tank is oscillating type, which can be move uniformly equal distance in both directions as a pair of rail track is fixed in the bottom for smooth movement of the bed.

A flume is fixed in the bed of the wave tank, which is shown in Figure 4. The length of the flume is 80.5cm, height is 13.5 cm and width is 22.5 cm. One grid of 1 cm square is attached on the flume to read the value of the flow profile at different point.

One scale is also fixed on the top of the flume to measure the oscillation and another scale fixed on the bed of the slope to read the value of the moving boundary. One side of the flume is fixed with a rigid vertical wall where as in the other end of the flume has a constant slope of 11.3^0.

One mirror is fixed just above the flume (shown in figure 3) to locate the value of the moving boundary while using movie camera from the orthogonal view of the flume. Colored water is used and proper lighting was assured for betterment of analyzing flow profile. Special care was taken to locate the position of the flow accurately and to locate the position of the moving boundary at the edges due to flow running on both directions just before reaching the top.

Image processing technique was used to locate the position of the flow profile inside the grid to reduce the eye estimation error. Many trials had been given to find a uniform weakly nonlinear flow on the slope. The positioning of the video camera was poised just in the middle of the flume and bed elevation of the bed and moving camera made equal. By changing the different initial condition set the program we could change out wave period and oscillation of the flume.

The desire initial condition was achieved by giving many trials, using the same initial condition the experiment had been carried out several times to enhance its accuracy. Before reaching the pick some turbulence at the moving edge was observed and energy dissipation calculate was needed to match the simulation result with the actual phenomena of the experiment.

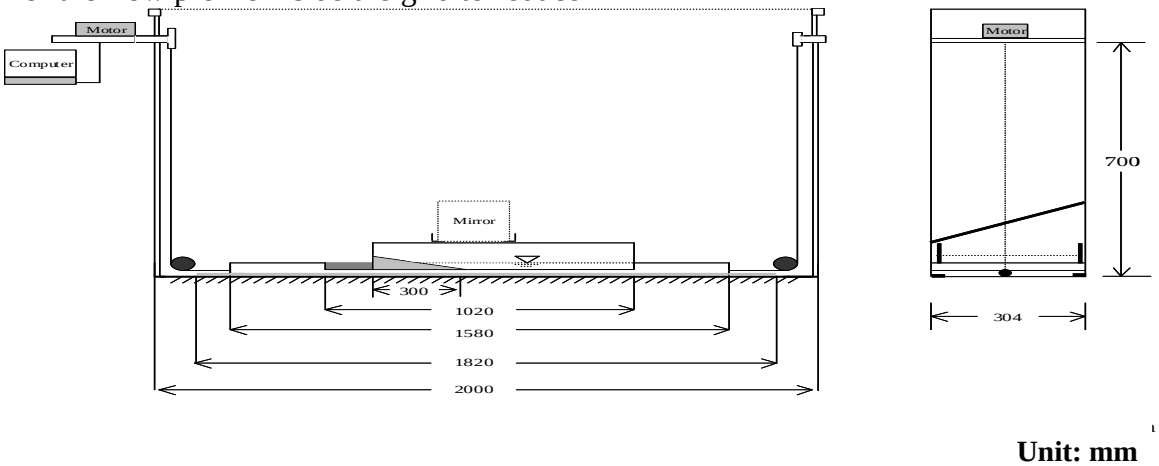

Figure 3. Dimensional sketch of the experimental setup

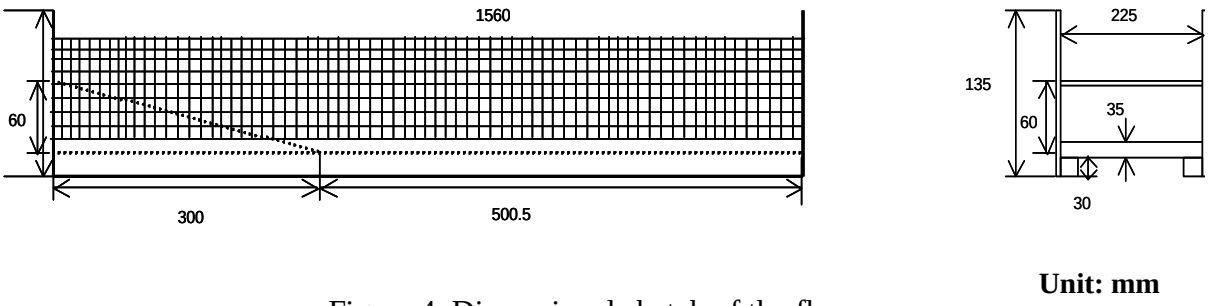

Figure 4. Dimensional sketch of the flume

3.2 Experimental results

From the experiment, it was found that the depth of water around 2 cm to 2.5cm, wave period of 3 to 3.5 sec produce desire flow profile on the slope. In the study case used depth of water is 2 cm, wave period is 3.5 second and oscillation of the flume is 6 cm.

Consistent 4 cm interval data of the whole flume was analyzed. The moving boundary varies 5.5 cm in its run-up and rundown process therefore amplitude variation of the wave is 1.1 cm which is quite big considering the initial water head, moreover before reaching the pick some turbulence at the moving edge was observed and energy dissipation calculate was needed to match the simulation result with the actual phenomena of the experiment.

Another important fact of this experiment is finding the uniform wave profile with respect to the moving flume. Figure 5 shows the variation of moving boundary with respect to the flume position. From this figure we can understand the initial high frequency flow is not uniform with the movement of the flume. After 10 sec of movement of the flume the variation of the moving boundary becomes uniform.

Figure 6 (a) to (d) of show the flow profile in run up and run down process on the sloping ground. From these figure we can understand more than one wave pick was found on the sloping ground in any instance of time. Consistent 4 cm interval data of the whole flume was analyzed. The moving boundary varies 5.5 cm in its run-up and rundown process therefore amplitude variation of the wave is 1.1 cm which is quite big considering the initial water head, moreover before reaching the pick some turbulence at the moving edge was observed and energy dissipation calculate was needed to match the simulation result with the actual phenomena of the experiment.
Most of previous approaches made by many authors the use gauge to measure the depth of at some interval points therefore there is a possibility not to have consistent data but in the present study we use 4 cm uniform interval throughout the whole flume which good consistence data throughout the whole flume.

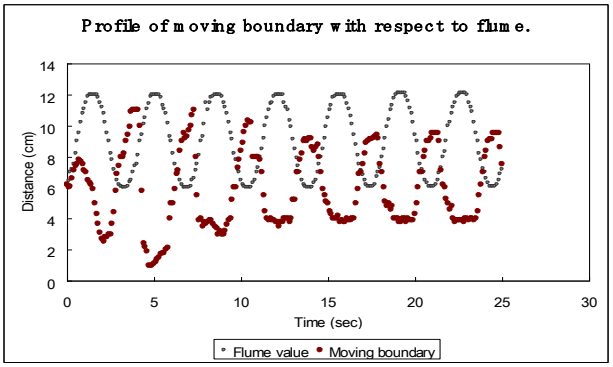

Figure 5. Variation of moving boundary with flume

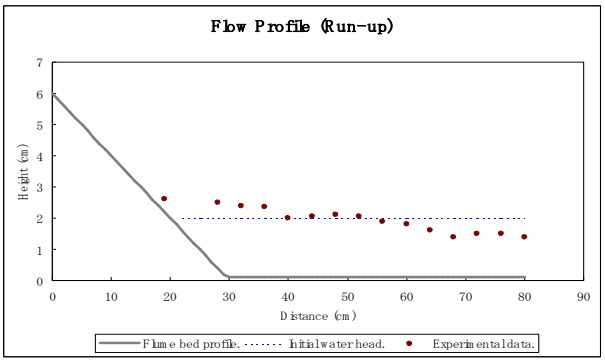

(a)

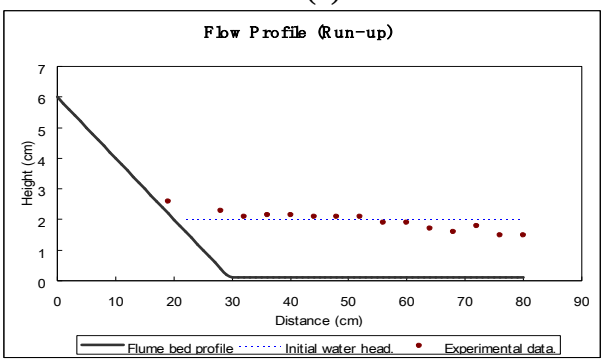

(b)

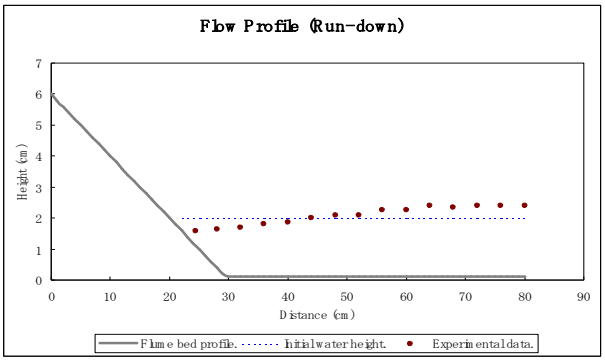

(c)

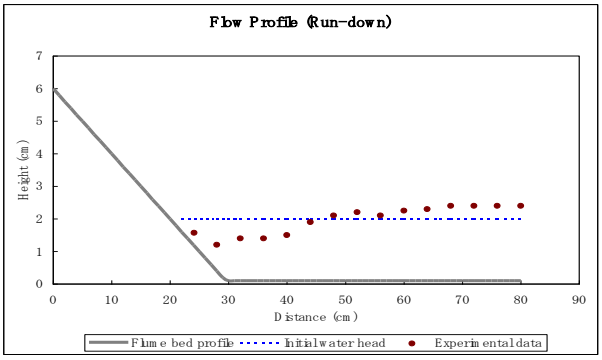

(d)

Figure 6. Flow profile in run up and rundown process on the sloping ground

4. VALIDATION OF THE MODEL

Many previous studies have applied shallow-water equations to solve the problem with a moving boundary, Carrier and Greeenspan (1958), Sielecki and Wurtele (1970), Gopalakrishnan and Tung (1983) R.S.Prasad, I.A.Svendsen (2003). Using the present model surface waves shoaling on a slope was solved successfully by comparing with the analytical solution derived by Carrier and Greenspan (1958). However, most of all previous studies have been verified by comparing with the theory, and the models have not been applied to reproduce the laboratory experiments whose results may include energy dissipation due to a wall and wave breaking. Therefore, we apply the proposed model to reproduce the laboratory experiment results by including the energy dissipation due to a wall and wave breaking.

4.1. Comparisons of results

Two tests were used to verify the proposed model, the time series of the location of a moving boundary and water level along a tank. We used the same parameters for the modeling of wave breaking in all cases. With regard to the time series of the location of a moving boundary, the computation and experiment results agreed well (Figure 7). Higher frequency waves were also found to occur with the same phase between the computations and experiments. However, the peak values from computations were slightly larger than the experiments while the stable cyclic variations appeared Figure 8 (a) to (f). It may be because of the surface tension effect. As the depth of water is only 2cm the effect affect significantly the outcome of the result (Desilva et al 1996).

The used value of the theoretical bottom friction for calculating wave breaking is another factor that might influences the results. The delay time of the flume at the two edges might also influence the outcome of the results moreover the eye estimation error due to measuring gauge is also another factor to need to be noted.

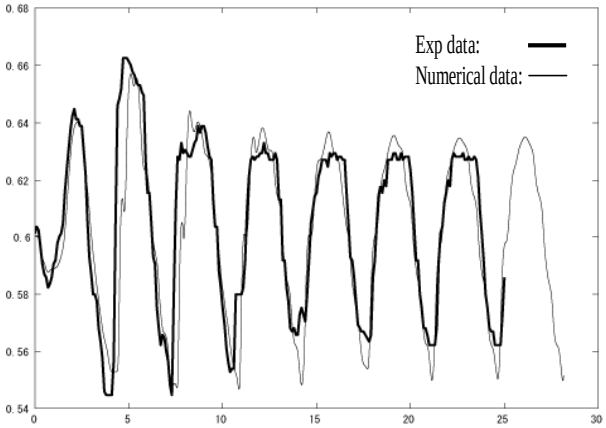

Figure 7. Time (s) vs height (cm) curve of the moving boundary

The following figure shows the comparison of the numerical and experimental data.

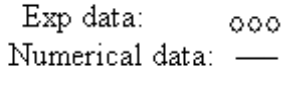

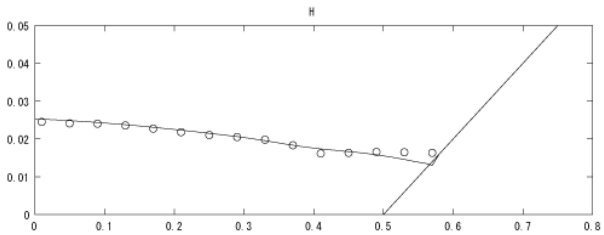

(a)

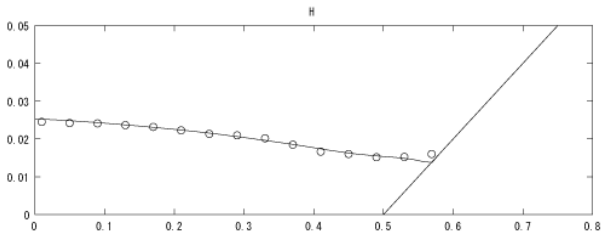

(b)

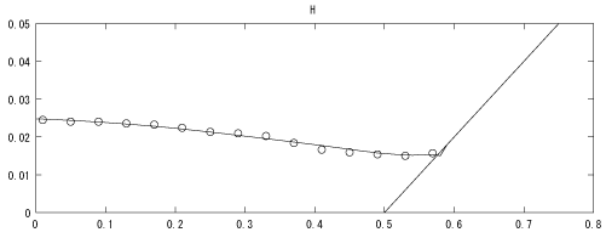

(c)

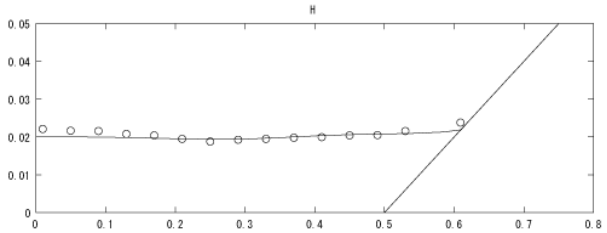

(d)

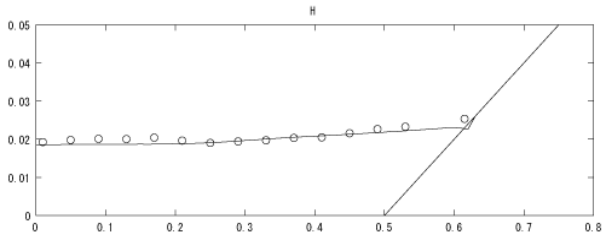

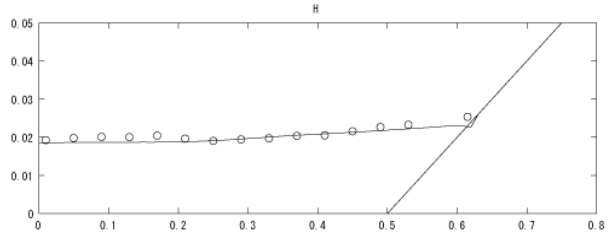

(e)

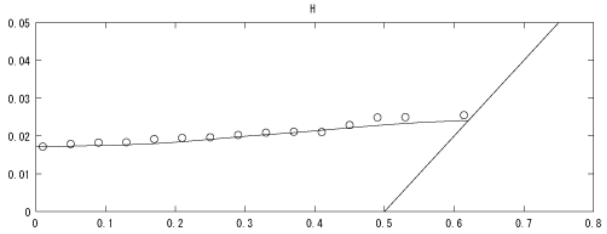

(f)

Figure 8. Run down and run up of long wave shoaling on to a sloping ground. Here distance of flow is in x directions whereas height of water is in y directions

4.2. Discussion of the results

Good agreements between the numerical simulation and laboratory experiment had been found. It should be noted that the parameters for wave-breaking model were determined from literatures in the numerical computations to reproduce the different experiment results with different conditions; the water depth, the oscillation period of the tank, and the amplitude of the oscillation.

Some errors may have appeared due to the lack of accuracy of the measuring gauge. The delay time of the flume at the two edges might also influence the outcome of the results. Adhesion force between water and flume due to surface tension also may reduce the agreement between computations and experiments.

4.3. Conclusion

At the time of the experiment, we observed the flume stopped for a fraction of seconds before moving to the opposite directions. Therefore, special attention was given to measure the location of the moving boundary.

Although high attention has been given to minimize eye estimation error, some irregularities of matching were found. Moreover, surface tension is quite significant at the edges because the water depth is relatively small with amplitude variation.

Although there were some irregularities between the numerical computation and experimental results, most part of the result from laboratory experiments agreed with computation results. Therefore, the proposed model could be applicable to solve wave-shoaling problem.

References

[1] K. Nakayama, K. Kudo and T. Ishikawa (2004): A new model to solve long waves shoaling on a sloping rectangular grids. *Journal of Hydraulic Engineering, JSCE,* 48,1.

[2] K. Nakayam, T. Ishikawa and K. Kudo (2000): IIM for surface waves shoaling on a slope. *International Journal for Numerical methods in Fluids* 00:1-6

[3] A. Balzano (1998) Evaluation of methods for numerical simulation of wetting and drying in shallow water flow models.. *Coastal Engineering* 34,83-107

[4] *P.J. Lynett, T.R. Wu, P.L.-F. Liu (2002)* Modeling wave run up with depth-integrated equations. *Coastal Engineering* 46, 89-107.

[5] B. Johns *(1982)* Numerical Integration of the shallow water equations over a sloping shelf. *International Jouranl for Numerical Methods in fluids*,2, 253-261.

[6] Sielecki, A; Wurtele, M.G (1970) The numerical integration of the nonlinear shallow-water equations with sloping boundaries. *Journal of Computational Physics*, 6, 2, 219-236.

[7] R.S. Prasad and I.A. Svendsen (2003) Moving Shoreline boundary condition for nearshore models. *Coastal Engineering*, 49, 4, 239-261.

[8] V.V. Titov and C.E. Synolakis (1998) Numerical Modeling of Tidal Wave Run up.. *Journal of Waterway, Port, Coastal, and Ocean Engineering/ July/August*, 157-171

[9] V.V. Titov, C.E.Synolakis (1995) Modeling of Breaking and Nonbreaking Long-wave evolution and Run-up using VTCS-2. *Journal of Waterway, Port and Coastal and Ocean Engineering, November/December* 308-316.

[10] A. Balzano (1998) Evaluation of Methods for numerical simulation of wetting and drying in shallow water flow models. *Coastal Engineering , 34, 1-2, 83-107*.

[11] T.C. Gopalakrishnan, C.C. Tung (1983) Numerical Analysis of a moving boundary problem in coastal hydrodynamics.. *International Journal for numerical methods in Fluids*, 3, 179-200.

[12] J.A. Zelt and F.Raichlen (1990)A Lagrangian model for wave-induced harbour oscillations. *J.Fluid Mech*, 213, 203-225.

[13] G. Pedersen and B. Gjevik (1983) Run-up of solitary waves. *J. Fluid Mech*, 135, 283-299

[14] P.L-F. Liu, Y. S.Cho, M.J.Briggs, U.Kanoglu, C.E. Synolakis (1995) Run-up of Solitary waves on a circular island. *J.Fluid Mech*, 302, 259-285

[15] Career and Greenspan. J (1958) Water waves of finite amplitude on a sloping beach. *Fluid Mech*. 17, 97-110.

[16] C.E.Synolakis (1987) The runup of solitary waves. *J.Fluid Mech*, 185, 523-545.

[17] A. Sielecki and M.G.Wurtele (1970) The numerical integration of the nonlinear shallow-water equations with sloping boundaries. *Journal of Computational Physics* 6, 219-236.

[18] W.C.Thacker. (1981) some exact solutions to the nonlinear shallow-water wave equations. *J.Fluid Mech*, 107, 499-508.

[19] N. W. Scheffner, L.E. Borgman, D.J.Mark (1996) Empirical Simulation Technique Based Strorm Surge Frequency Analyses *Journal of Waterway, Port, Coastal, and Ocean Engineering / March / April* 93-99.

[20] S.J.Desilva, R.B.Guenther and R.T.Hudspeth. Irregular points in 2-D free surface flows with surface tension for the wavemaker boundary value problem. *Applied Ocean Research* 18, 293-302.